



An analytical model to predict and minimize the residual stress of laser cladding process

N. Tamanna¹ · R. Crouch¹ · I. R. Kabir¹ · S. Naher¹

Received: 31 October 2017 / Accepted: 14 January 2018 / Published online: 2 February 2018
© The Author(s) 2018. This article is an open access publication

Abstract

Laser cladding is one of the advanced thermal techniques used to repair or modify the surface properties of high-value components such as tools, military and aerospace parts. Unfortunately, tensile residual stresses are generated in the thermally treated area of this process. This work focuses on to investigate the key factors for the formation of tensile residual stress and how to minimize it in the clad when using dissimilar substrate and clad materials. To predict the tensile residual stress, a one-dimensional analytical model has been adopted. Four cladding materials (Al_2O_3 , TiC, TiO_2 , ZrO_2) on the H13 tool steel substrate and a range of preheating temperatures of the substrate, from 300 to 1200 K, have been investigated. Thermal strain and Young's modulus are found to be the key factors of formation of tensile residual stresses. Additionally, it is found that using a preheating temperature of the substrate immediately before laser cladding showed the reduction of residual stress.

1 Introduction to the style guide

Laser cladding (LC) is one of the advantageous thermal techniques over thermal spraying, plasma spraying and arc welding [1]. In this process, a laser heat source is used to deposit a thin layer, mostly at micro-scale, of a desired material on a substrate material [2]. One of the challenges of this process is the formation of tensile residual stresses in the thermally treated area [3–5]. Residual stresses are the locked in stress in any engineering components after thermal or mechanical treatment in the absence of any external load [6]. These residual stresses deteriorate the performance of engineering components such as fatigue life [7], corrosion resistance [8] and dimensional accuracy [9] in the finished products. A one-dimensional analytical model was proposed to predict the stress evolution considering elastic, plastic and thermal strain [10]. To predict the tensile residual stress, a

simplified analytical model was established based on the elastic mechanics for dissimilar materials by Wang et al. [3]. Numerical methods are applied to calculate three-dimensional state of residual stresses in the treated object. Mainly, tensile residual stresses were predicted on the surface while the quantity of these stresses was different in different directions, along with experimental validation [4]. The fundamental understanding of the formation of residual stress in dissimilar material is not well established because of the lack of knowledge about materials' behaviour in the process. Models are focused on the same cladding and the substrate material [11]. In some cases, dissimilar cladding and substrate materials have been examined [4]. However, these models and experimental works do not explain the effect of different properties of cladding materials on residual stresses when the same substrate material was used. Doping is a popular method to improve materials properties by intentionally introducing impurities in the substrate. It is found from doping mechanism that residual stresses varied when dissimilar doping materials were used [12]. Other thermal cladding process such as thermal spray [13] and plasma spray [14] showed the differences of residual stress for different cladding materials on the same substrate. Recently, to minimize residual stresses, deposition of functionally graded material are used. This process can minimize the differences of mismatch of thermal strain between materials [15]. So, it is required to develop an understanding of the influence of materials properties on the formation of residual stresses.

✉ N. Tamanna
Nusrat.Tamanna@city.ac.uk

R. Crouch
Roger.Crouch.1@city.ac.uk

I. R. Kabir
Israt.Kabir.1@city.ac.uk

S. Naher
Sumsun.Naher.1@city.ac.uk

¹ City, University of London, Northampton Square,
London EC1V 4HB, UK

The high temperature gradient from the clad to the substrate material is one of the main reasons for the formation of cracks. The higher cooling rate generates higher misfit of strain, resulting higher residual stress [13]. Preheating of the substrate reduces the thermal gradient which significantly minimizes residual stresses and prevents cracks on the surface [16].

In this work, an analytical model is presented to calculate the tensile residual stress in dissimilar materials. Four widely used cladding materials have been used to observe the change of residual stresses on the H13 tool steel substrate which is a popular material for tooling application [17]. This technique provides a unique method to compare residual stresses for different cladding materials, with capabilities to integrate material properties. Furthermore, preheating temperature of the substrate was applied to check the effect on residual stresses.

2 Methodology

H13 tool steel was used as a substrate material and Al₂O₃, TiC, TiO₂ and ZrO₂ were used for cladding materials. The preheating temperature of substrate was varied from 300 to 1200 K. The material properties are given in Table 1.

A simplified model was adopted to calculate the residual stress as shown in Fig. 1 considering the elastic and the thermal strain. σ is the normal tensile residual stress [3, 22]. α , E and h are defined as the thermal expansion coefficient, Young’s modulus and thickness, respectively. The subscripts c and s represent the clad and the substrate, respectively. T_r , T_o and T_{mc} are room temperature, preheating temperature of the substrate and melting temperature or operating temperature of cladding materials, respectively. In the laser cladding process, the operating temperature should be equal or more than the melting temperature of cladding materials. If the clad and the substrate contract freely, the thermal contractions are $\alpha_c l (T_{mc} - T_r)$ and $\alpha_s l (T_o - T_r)$ correspondingly. The higher thermal strain of cladding material was assumed than the substrate material, see Fig. 1. The induced elastic strains are σ_c/E_c and σ_s/E_s due to

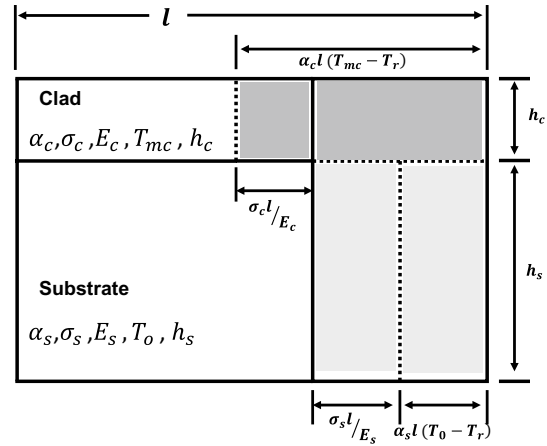


Fig. 1 The geometry of residual stress model based on thermo-elastic mechanics [3]

residual stress of clad and the substrate. However, the coating and the substrate are connected with a metallurgical bonding. So the actual contraction at the interface of the clad and the substrate is

$$\alpha_c l (T_{mc} - T_r) - \sigma_c l / E_c = \alpha_s l (T_o - T_r) + \sigma_s l / E_s \tag{1}$$

The uniform stress distribution is assumed in the clad and the substrate while the height of the clad was lower than the height of the substrate. From the internal force balance,

$$h_s \sigma_s = h_c \sigma_c, \tag{2}$$

where h_s and h_c are the heights of the substrate and the clad, respectively. σ_c and σ_s are the tensile residual stresses of the clad and the substrate. From Eq. 1 and Eq. 2, the generated stress in the clad can be derived,

$$\sigma_c = \frac{h_s E_s E_c [\alpha_c (T_{mc} - T_r) - \alpha_s (T_o - T_r)]}{h_s E_s + h_c E_c} \tag{3}$$

Table 1 Material properties used to calculate the residual stress

Materials	Thermal expansion coefficient $\times 10^{-6}(\text{K}^{-1})$	Young’s modulus (GPa)	Melting temperature (K)	Height (m)
H13 tool steel ^a	10.90 [4]	210	1752	0.005*
Al ₂ O ₃ ^b	5.40 [18]	380	2338	0.001**
TiC ^b	7.70 [19]	449	3363	0.001**
TiO ₂ ^b	11.80 [20]	288	2123	0.001**
ZrO ₂ ^b	12.20 [21]	250	2973	0.001**

^aSubstrate material

^bCladding materials

Height of the substrate (*) and height of the clad (**)

The effect of different materials and preheating temperature of the substrate on the generation of residual stresses were theoretically investigated using this model. The results of residual stresses are normalized with the residual stress of TiC clad. Thermal strain of the material is related with the thermal expansion coefficient of materials and temperature difference of the operating temperature and the room temperature. The mismatch of the thermal strain between the clad and the substrate ($\alpha_c(T_{mc} - T_r) - \alpha_s(T_0 - T_r)$ in Eq. 3) was found one of the reasons of formation of residual stresses in the system. Another material property, Young’s modulus (E_c in Eq. 3), was considered with the mismatch of thermal strain to understand its effect on the formation of residual stress.

3 Results and discussion

Figure 2 shows the distribution of predicted tensile residual stresses for different cladding materials (Al_2O_3 , TiC, TiO_2 , ZrO_2) on the H13 tool steel substrate at a range of preheating temperature (300 to 1200 K) of the substrate. TiC cladding material formed higher residual stress than TiO_2 cladding material. The minimum residual stress was formed for Al_2O_3 cladding material. TiC cladding material formed the maximum tensile residual stress below 900 K preheating temperature of the substrate, while ZrO_2 cladding material formed the maximum tensile residual stress above 900 K preheating temperature of the substrate, see Fig. 2. The predicted residual stress of four cladding materials at 300 K and at 1200 K preheating temperature of the substrate is shown in Fig. 3a, b, respectively. To understand the variation of residual stresses for different material system, thermal strain and Young’s modulus have been analysed.

The mismatch of thermal strain, $\alpha_c(T_{mc} - T_r) - \alpha_s(T_0 - T_r)$ in Eq. 3, between the clad and the substrate material is one of the reasons of the formation of residual stress. The differences of the thermal strain of four cladding materials from the substrate material are shown in Fig. 4a, b at the 300 and 1200 K preheating temperature of the substrate, respectively.

ZrO_2 cladding material showed higher mismatch of thermal strain with the substrate at any preheating temperature than other clad materials, see Fig. 4a, b. However, below 900 K preheating temperature of the substrate, TiC cladding material generated higher tensile residual stress than ZrO_2 cladding material. To clarify this issue, another material property, Young’s modulus, was considered. The Young’s modulus of TiC and ZrO_2 cladding materials is 449 GPa and 380 GPa, respectively. From Eq. 3, we have taken the

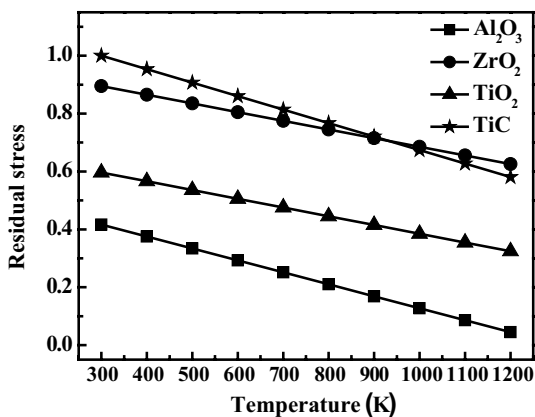


Fig. 2 Distribution of the normalized residual stress with preheating temperature of the substrate for four cladding materials

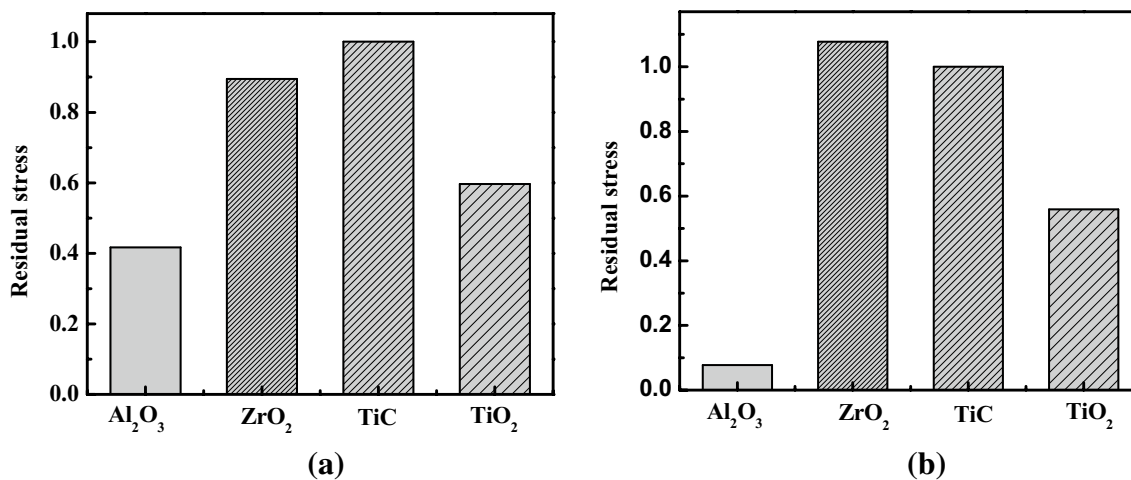


Fig. 3 The normalized residual stress a at 300 K and b at 1200 K preheating temperature of the substrate for four cladding materials

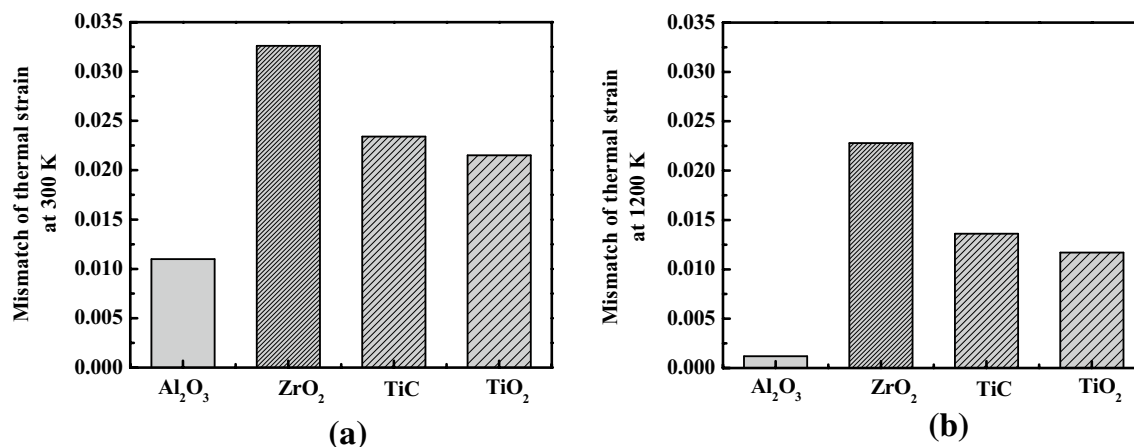


Fig. 4 Mismatch of thermal strain between the cladding materials and the substrate **a** at 300 K and **b** at 1200 K preheating temperature of the substrate

part related with mismatch of thermal strain and Young’s modulus of clad material, $E_c [\alpha_c (T_{mc} - T_r) - \alpha_s (T_0 - T_r)]$, to explain this trend. The product of mismatch of thermal strain and Young’s modulus was shown in Fig. 5a, b. At 300 K, TiC cladding material showed maximum value shown in Fig. 5a. Moreover, TiC has higher Young’s modulus and very small difference between mismatch of thermal strain with ZrO₂. However, mismatch of thermal strain was decreased with increasing the preheating temperature of the substrate. The degree of decrement of the mismatch of thermal strain between TiC cladding material and the substrate was higher than ZrO₂ cladding material above 900 K generating lower residual stress, though the Young’s modulus of TiC was higher.

If we compare between Al₂O₃ and ZrO₂ cladding materials, the Young’s modulus of Al₂O₃ (380 GPa) cladding

material is higher than ZrO₂ (250 GPa) cladding material. However, ZrO₂ cladding material produced higher residual stress. Then, it is important to focus on the mismatch of thermal strain. The mismatch of thermal strain of Al₂O₃ is much lower than ZrO₂ which generating lower residual stress in Al₂O₃ cladding material.

The residual stress decreased with the rise of the preheating temperature of the substrate for all types of cladding materials. The reason behind the descendant trend of the residual stress is the lower thermal gradient between the clad and the substrate material and relatively slower cooling rate [16, 23]. The slower the cooling rate, the material got longer time to come back to the original dimension. As it takes longer time to come back to room temperature, the mismatch of thermal strain also decreased between two materials.

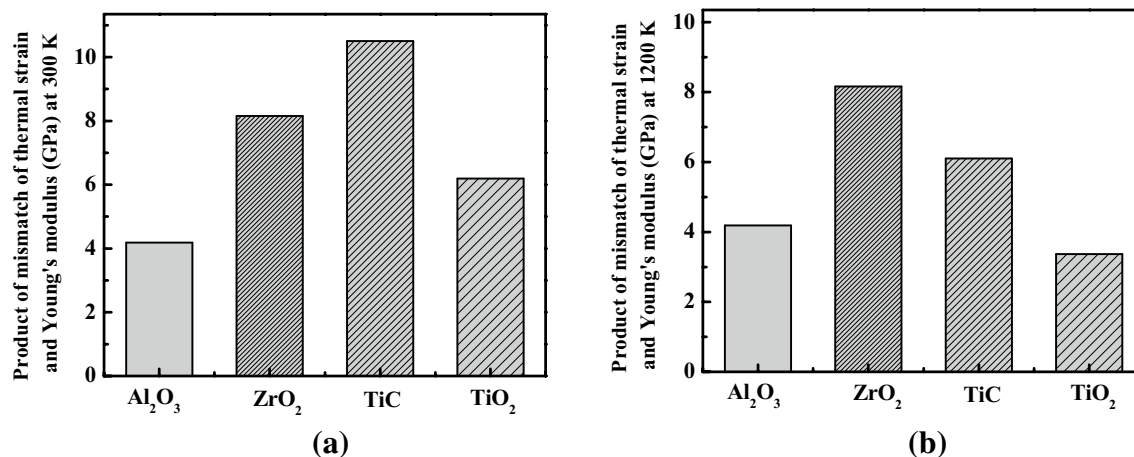


Fig. 5 Product of mismatch of thermal strain and Young’s modulus **a** at 300 K and **b** at 1200 K preheating temperature of the substrate for four cladding materials

4 Conclusions

An analytical model has been used to calculate and compare the stress generation in dissimilar clad and substrate material system with different preheating temperatures of the substrate. Four cladding materials, TiO_2 , TiC , ZrO_2 and Al_2O_3 were used on the H13 tool steel substrate. Below 900 K preheating temperature of the substrate, maximum residual stress was generated in the TiC clad. The maximum residual stress was formed in ZrO_2 clad above 900 K. The minimum residual stress was found for Al_2O_3 clad. Thermal strain and Young's modulus were found as key factors of the generation of residual stress. The minimum mismatch of thermal strain was found in Al_2O_3 clad. The reduction of mismatch of thermal strain can reduce the residual stress in the clad. This analysis can be used to find a combination of materials that can generate minimum residual stress. This model is capable to include preheating of the substrate and predicts its effect on the distribution of the residual stress. The increment of preheating temperature of substrate decreased the residual stress.

Acknowledgements Sincere thanks to EU funded Erasmus Mundus project, EM LEADERS reference: 551411-EM-1-2014-1-UK-ERA MUNDUS-EMA21_EM, and School of Mathematics, Computer Science and Engineering of City, University of London for funding the Project.

Open Access This article is distributed under the terms of the Creative Commons Attribution 4.0 International License (<http://creativecommons.org/licenses/by/4.0/>), which permits unrestricted use, distribution, and reproduction in any medium, provided you give appropriate credit to the original author(s) and the source, provide a link to the Creative Commons license, and indicate if changes were made.

References

1. E. Toyserkani, A. Khajepour, S.F. Corbin, *Laser Cladding*, 1st edn. (CRC Press, New York, 2004)
2. C.S. Chien, C.W. Liu, T.Y. Kuo, C.C. Wu, T.F. Hong, *Appl. Phys. A Mater. Sci. Process.* **122**, 1 (2016)
3. D. Wang, Q. Hu, X. Zeng, *Surf. Coatings Technol.* **274**, 51 (2015)
4. P. Farahmand, R. Kovacevic, *Opt. Laser Technol.* **63**, 154 (2014)
5. N. Tamanna, R. Crouch, S. Naher, 20th Int. ESAFORM Conf. Mater. Form. **40015**, (2017)
6. M. Eslami, R. Hetnarski, J. Ignaczak, N. Noda, N. Sumi, *Theory of Elasticity and Thermal Stresses*, 1st edn. (Springer, New York, 2013)
7. Y. Chew, J.H.L. Pang, *Int. J. Fatigue.* **87**, 235 (2016)
8. A. Martinez Hurtado, J.A. Francis, N.P.C. Stevens, *Mater. Sci. Technol.* **32**, 1484 (2016)
9. J. Liu, L. Li, *Opt. Laser Technol.* **36**, 477 (2004)
10. F. Brückner, D. Lepski, E. Beyer, *J. Therm. Spray Technol.* **16**, 355 (2007)
11. M. Hao, Y. Sun, *Int. J. Heat Mass Transf.* **64**, 352 (2013)
12. P. Han, F.R. Xiao, W.J. Zou, B. Liao, *Ceram. Int.* **40**, 5007 (2014)
13. T.W. Clyne, S.C. Gill, *J. Therm. Spray Technol.* **5**, 401 (1996)
14. J. Matejicek, S. Sampath, P.C. Brand, H.J. Prask, *Acta Mater.* **47**, 607 (1999)
15. Z. He, J. Ma, G.E.B. Tan, *J. Alloys Compd.* **486**, 815 (2009)
16. Y.-F. Tao, J. Li, Y.-H. Lv, L.-F. Hu, *Opt. Laser Technol.* **97**, 379 (2017)
17. F. Klocke, K. Arntz, M. Teli, K. Winands, M. Wegener, S. Oliari, *Procedia CIRP.* **63**, 58 (2017)
18. P. Auerkari, *Mechanical and Physical Properties of Engineering Alumina Ceramics*, Technical Research Centre of Finland, VTT Manufacturing Technology, Research Notes 1792, 3–36 (1996)
19. D.Y. Dang, J.L. Fan, H.R. Gong, *J. Appl. Phys.* **116**, 0 (2014)
20. AZoM (2002), <https://www.azom.com/article.aspx?ArticleID=1179>. Accessed 31 Oct 2017
21. AZoM (2002), <https://www.azom.com/properties.aspx?ArticleID=133>. Accessed 31 Oct 2017
22. F.P. Incropera, T.L. Bergman, A.S. Lavine, D.P. DeWitt, *Fundamentals of Heat and Mass Transfer*, 7th edn. (Don Fowley, Jefferson, 2011)
23. S. Zhou, X. Dai, H. Zheng, *Opt. Laser Technol.* **43**, 613 (2011)